ELSEVIER

Journal of Power Sources 92 (2001) 9–16

JOURNAL OF POWER SOURCES

www.elsevier.com/locate/jpowsour

A parametric study of fuel cell system efficiency under full and part load operation

Bernt Thorstensen*

KeraNor AS, Brobekkveien 104A, N-0582 Oslo, Norway

Received 19 August 1999; received in revised form 20 October 1999; accepted 17 April 2000

Abstract

Fuel cell technology is an emerging, environmentally friendly energy conversion technology for use in mobile and stationary applications. A contribution to the understanding of fuel cell system efficiency and operation under full and part load is presented in this paper. An analytical, three-parameter model, independent of specific fuel cell system, is developed and important performance parameters defined and discussed. Three useful properties of fuel cells are documented: (i) their ability to produce electric energy with constant — or even increased — efficiency at reduced power (enhanced part power efficiency), (ii) their ability to respond instantaneously to changes in power delivery demands (instantaneous load-following properties), and (iii) their theoretical ability to deliver an exhaust gas consisting of almost pure CO_2 (intrinsic CO_2 separation).

Keywords: Fuel cells; Efficiency; System; Load-following properties; CO_2-separation; Performance parameters; Mathematical model; Data

1. Introduction

1.1. Background

The British scientist Sir William Robert Grove [1] invented the fuel cell about 160 years ago. However, first in the 1960s another British scientist, F.T. Bacon and co-workers [2], succeeded in demonstrating the first effective and useful cell. This was a fuel cell with alkaline electrolyte, and the concept was readily transferred to the United States space program. Nevertheless, fuel cell technology has not yet been developed to a mature and competitive option for the world energy conversion market.

However, there has been a growing interest for fuel cells in the last few decades. A multitude of fuel cell demonstration systems have been developed, and large governmentally funded development programs are being conducted in many of the industrialised countries around the world, particularly in North America, Europe and Japan. Commercial fuel cell prototypes or units are available in the open market today, although they are still not price competitive with other energy conversion devices. Nevertheless, many have the expectation that the fuel cell technology within the near future will manifest itself as a competitive and environment-friendly energy conversion technology for use in mobile as well as stationary applications.

For the future *users* of fuel cell technology a systematic and uniform description of the behaviour of fuel cell systems will be helpful in order to give him the opportunity to select the right fuel cell type, the right brand, and the right operating conditions. The future *manufacturers* of fuel cells will have the same need for a uniform description in order to communicate with potential customers. The future fuel cell *developers* also need this description in order to be able to attack the essential parameters for improvements.

Therefore, there is a need for unification of performance data and product information for fuel cell systems. The present article deals with this. A generic, analytical model, describing the energy efficiency of fuel cells under full and part load operation is developed, and important performance parameters are defined and discussed. This user-oriented model is independent of the specific fuel cell system in use. Since there are limited data available for fuel cell systems in operation, the model has so far only been tested with performance data from a commercial PAFC system.

1.2. Fuel cell classification

Fuel cells are classified by their electrolyte type. Of the four different, advanced fuel cell types that today are under development, two have liquid electrolytes (phosphoric acid,

* Tel.: +47-22-88-13-20; fax: +47-22-88-13-21.

0378-7753/01/$ – see front matter
PII: S0378-7753(00)00497-3

molten carbonate) and two have solid electrolytes (solid polymer, solid oxide).

The choice of the electrolyte also determines the operating temperature. Generally, solid polymer fuel cells are recognised as *low-temperature* (90°C), phosphoric acid fuel cells as *intermediate-temperature* (200°C), and molten carbonate and solid oxide fuel cells as *high-temperature* (650–1000°C) fuel cells. However, fuel cells with solid polymer electrolytes operating above 100°C, and solid oxide electrolytes operating below 700°C are also interesting development lines.

Detailed description of the different fuel cell types and their operation can be found in [3–5].

2. Fuel cell system efficiency

The fuel cell system efficiency depends on the system selected, the operating conditions, i.e. temperature, pressure and fuel used, and also on the system specific technical components and balance of plant (BOP) solutions.

The efficiency of the fuel cell itself has a maximum theoretical value η_{max} for zero power delivery, given by

$$\eta_{max} = \frac{\Delta G_T}{\Delta H_0}, \tag{1}$$

where ΔG_T is the change in free energy of the electrochemical oxidation of the fuel, and ΔH_0 is the enthalpy change for the total oxidation reaction of the fuel.

When electric power is produced, losses in the fuel cell reduce the actual cell efficiency. Assuming the linear current–voltage characteristic of Fig. 1, the cell voltage U can be expressed as

$$U = \eta_v \times E_{rev} \tag{2}$$

where η_v is the voltage efficiency and E_{rev} denotes the reversible cell voltage or idealised open cell voltage, given by

$$E_{rev} = \frac{-\Delta G_T}{n_e F} \tag{3}$$

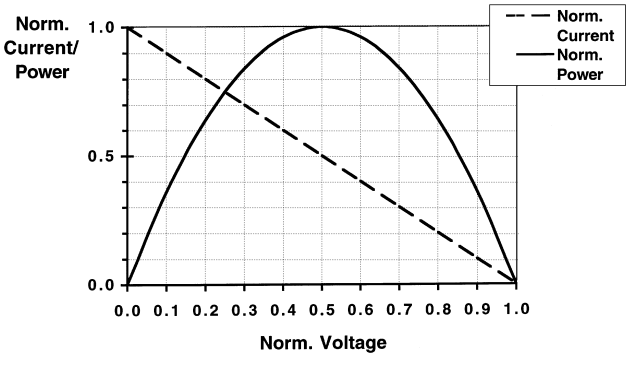

Fig. 1. Idealised current/voltage- and power/voltage-characteristics (normalised). For practical fuel cell operation, only the right-hand side of the diagram (normalised voltages>0.5) is used.

where n_e is the number of electrons per molecule participating in the electrochemical process, and F denotes the Faraday constant. The assumption about the linearity of the current–voltage characteristic, is independent of the specific fuel cell system.

If electrons are produced with a 100% Faradaic efficiency, the produced output power yields

$$P = UI = E_{rev} I_0 (1 - \eta_v)\eta_v = 4P_{max}(1 - \eta_v)\eta_v \tag{4}$$

where I_0 is the short circuit current and P_{max} denotes the *maximum power*, obtained for the value of η_v equals one-half.

An important fuel cell parameter is the rated or *nominal power output* (P_{nom}) which generally will be less than the theoretical maximum value (P_{max}). The ratio between these two parameters is defined as the *peak power capacity* (p_{pc}):

$$P_{max} = p_{pc} P_{nom} \tag{5}$$

Defining the normalised power output p as

$$P = \frac{P}{P_{nom}} \tag{6}$$

Eq. (4) can be solved for η_v as a function of p to yield

$$\eta_v = \frac{1 + \sqrt{1 - p/p_{pc}}}{2} \tag{7}$$

The total cell efficiency (η_{cell}) is defined as

$$\eta_{cell} = \eta_v \times \eta_{max} \tag{8}$$

For the fuel cell system, the fuel efficiency η_{fuel} is defined as

$$\eta_{fuel} = u_{fu} \times u_{ref} \tag{9}$$

where u_{fu} is the *fuel utilisation* and u_{ref} is the fuel processing or *reformer efficiency*.

For the fuel cell system operation there is several sources for parasitic losses, e.g. fans, blowers, heat exchangers, electric control system, etc. As a first approximation, a linear relationship is assumed between the parasitic power losses P_{para} and power output:

$$P_{para} = \alpha_0 + \beta_0 P \tag{10}$$

where α_0 is the *stand-by losses* and β_0 is the normalised *operational dependent losses*. The parasitic efficiency η_{para} is then

$$\eta_{para} = \frac{P - P_{para}}{P} = \frac{(1 - \beta_0)p - \alpha_1}{p} \tag{11}$$

by substitution of Eq. (10), and where

$$\alpha_1 = \frac{\alpha_0}{P_{nom}}. \tag{12}$$

is the normalised stand-by losses.

In addition the electric interface losses have to be accounted for. The balance of plant efficiency (η_{BOP}) is defined as

$$\eta_{BOP} = \eta_{el} \times \eta_{para} \tag{13}$$

where η_{el} is the (DC-AC, or DC-DC) *electric conversion efficiency*. The total fuel cell system efficiency (η_{TOT}) is then

$$\eta_{TOT} = \eta_{cell}\eta_{fuel}\eta_{BOP} = \eta_{el}u_{fu}u_{ref}\eta_{max}\frac{(1-\beta_0)p-\alpha_1}{p} \times \frac{1+\sqrt{1-p/p_{pc}}}{2} \quad (14)$$

Since the different efficiencies may be difficult to determine separately, parameters may be aggregated, to yield the generalised equivalent of Eq. (14):

$$\eta_{TOT} = F(p) \times \frac{1+\sqrt{1-p/p_{pc}}}{2} \quad (15)$$

where $F(p)$ is the generalised system *efficiency function*, with the linearisation of Eq. (10) as a special case, yielding

$$F(p) = \lambda_0 + \frac{\lambda_1}{p}. \quad (16)$$

From Eq. (14) we find the expression for the aggregated system efficiency factor λ_0:

$$\lambda_0 = \eta_{el}u_{fu}u_{ref}\eta_{max}(1-\beta_0) \quad (17)$$

and the aggregated system first-order loss factor λ_1

$$\lambda_1 = -\eta_{el}u_{fu}u_{ref}\eta_{max}\alpha_1 \quad (18)$$

Eq. (15) with the use of the linearised Eq. (16), yields a three-parameter description of the fuel cell efficiency under full and part load operation.

The generalised system efficiency function $F(p)$ may be developed to the second or higher order by an asymptotic expansion in the variable $1/p$. Results for the second-order expansion are given in Appendix A.

3. Discussions

The assumption about the linearity of the current–voltage characteristic, is independent of the specific fuel cell system, hence the developed mathematical model is true system-independent and can be applied to any of the fuel cell systems and types.

Since there are limited amount of available data covering true industrial systems running with a controlled fuel utilisation, the model has only been tested towards a commercial phosphoric acid fuel cell (PAFC) system [6]. This is illustrated in Fig. 2. By using values of 58.3% for the efficiency factor, −7.4% for the first-order loss factor, and 180% for the peak power capacity, the fit was better than ±10% for power levels down to 20% of the nominal power output.

Other types of fuel cell systems can be described with the similar set of parameters. However, each system has to be analysed and its specific parameters determined.

A brief discussion about fuel cell fuels and fuel processing, as well as the parameters of Eqs. (14)–(16) follows below. The values indicated for the different parameters are rough estimates based on the author's experience and included as indicators or examples. Also the enhanced part power efficiency, the instantaneous load-following properties, and the intrinsic CO_2-separation abilities of fuel cells are discussed.

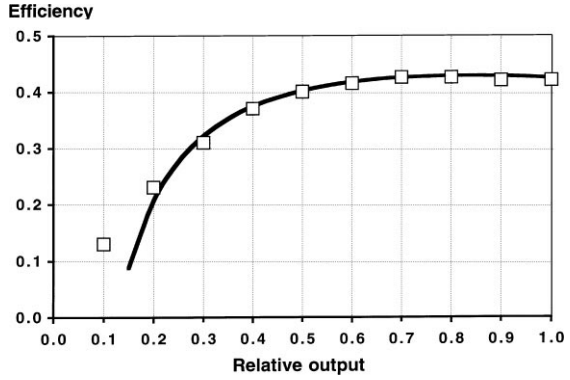

Fig. 2. Calculated fuel cell system efficiency as a function of normalised power output for a commercial phosphoric acid fuel cell (PAFC) system, when reformed natural gas is used as fuel, based upon data from Sydkraft [6], shown as open squares. The calculation (solid line) is based upon the three parameter model of Eq. (15) with the values 58.3% for the system efficiency factor, of −7.4% for the first-order loss factor, and 180% for the peak power capacity.

3.1. Fuel cell fuels

3.1.1. Fuel selection

Fuel cells are in general flexible with respect to the choice of fuel. For transportation applications the fuel logistics and availability is of particular importance, whereas for stationary applications the abundance of the fuel is important. The following are the most likely near term candidates for fuel cell applications:

1. *Hydrogen*: is the ideal fuel for fuel cells since no stage of fuel processing is required. Although it may be the ultimate solution as worldwide energy carrier, no large-scale production and distribution systems exist today (although hydrogen is produced at large quantities for industrial purposes). Problems related to the high diffusivity of hydrogen through most materials, metal hydride formation, and the explosive hazard of hydrogen have to be addressed.

   For most industrial applications today, hydrogen is produced from natural gas by reformation. However, more than 5% of the original energy in the natural gas is lost in this process [7]. Hydrogen produced by photothermal/photocatalytic splitting or nuclear powered electrolysis of water may become the ultimate solution.
2. *Natural gas*: may be a near term alternative as fuel cell fuel, due to its abundance and purity. Pipe lines and distribution networks exist world wide for natural gas. Natural gas may be stored either compressed (CNG) or liquefied (LNG). With respect to volume and energy

density, LNG has the preferred properties, although liquefaction incurs an energy penalty.

Natural gas may be processed to hydrogen, methanol, or diesel fuel (sulphur free). However, for the two last fuels up to 40% of the original energy in the natural gas is lost [8], so preferably the natural gas should be used directly.

3. *Methanol*: has by many been considered as the successor of petrol and diesel oil for transportation purposes. Since methanol is liquid at room temperature and atmospheric pressure, the existing distribution system for petrol and diesel oil may be used. However, the toxicity of methanol may be of concern.

   Methanol may be produced from biomass or natural gas, with the latter as the main source today. With the high energy losses in the conversion from natural gas, see above, biomass should be the preferred method of methanol production for the future.

   Methanol is in principle easier to reform than NG, i.e. lower temperatures are needed. For low-temperature fuel cells with increased operating temperature (150°C) internal or integrated reformation can take place, see Section 3.1.2 below.

   Other alcohols have also been regarded as potential energy carriers, particularly ethanol. For the purpose of this article ethanol has very similar properties compared with methanol, and is hence interchangeable with methanol with the exception of methanol's toxicity.
4. *Diesel oil*: exists in various grades (qualities) and is the most abundant and easily available fuel for transportation (both land based and marine) applications today. Diesel oil has a high energy content per unit volume.

   Since fuel cells in general are sensitive to sulphur contamination of the fuel, diesel oil will have to be desulphurised before use.

Table 1 summarises some techno-economical data for these fuels.

3.1.2. Fuel processing

The choice of fuel and fuel cell system will influence the handling and the processing of the fuel. This may again influence the total system costs, the operating costs and efficiency.

The processing of hydrocarbon fuels generally consists of steam reforming followed by a shift reaction. This converts the hydrocarbons into hydrogen that can be directly fed into all types of fuel cells. With methane (CH_4) as an example of a hydrocarbon fuel (natural gas), the sum of these two processes yields

$$CH_4 + 2H_2O = CO_2 + 4H_2. \quad (19)$$

These processes take place on catalysts, e.g. nickel at elevated temperatures. The ratio of steam to methane, together with the process conditions (temperature, pressure), determine the composition of the product gas. There are three different ways to implement the reformation processes in a fuel cell system:

1. *External reformation* (ER) with the process equipment outside the fuel cell stack. This is the solution for most of the low- and intermediate-temperature fuel cells, since the reformation process temperature generally is significantly higher than the fuel cell operating temperature. Often gas cleaning processes must follow the reformation steps, since particularly the low-temperature fuel cells are sensitive to traces of certain product species (e.g. CO).
2. *Internal reformation (IR)* with the process equipment thermally integrated in the fuel cell stack. Can be used with all the high-temperature fuel cells and reduces external thermal losses.
3. *Direct integrated reformation* (DIR) where the fuel cell anode acts as the reforming element. Can be used with all the high-temperature fuel cells and ensures excellent thermal coupling. The potential drawback is that the thermal coupling may be too high creating strong thermal gradients in the fuel cell stack due to the endothermic reformation reaction. Cleaning of the reformed gas is not possible, and the chance for a detrimental coke formation and deposition on the fuel cell electrode is enhanced.

3.1.3. The fuel reaction in the fuel cell

The hydrogen generated in the reformation process (Eq. (19)) can then be electrochemically oxidised in the fuel cell, as

$$4H_2 + 4O^{2-} = 4H_2O + 8e^- \quad (20)$$

Table 1
Data for alternative fuels for fuel cells [9–11]

Fuel	Density (g/cm^3)	Energy content (MJ/l)	Volume per energy unit relative to CNG (%)	Cost per MW h relative to CNG (%)	CO_2 emission penalty relative to CNG (%)
H_2 (200 atm)	0.02	2.8	245	225	0
CNG (200 atm)	0.14	6.8	100	100	100
LNG (−160°C)	0.46	22.3	30	115	110
Methanol	0.79	17.8	39	165	122
Diesel	0.85	38.5	18	140	130

(assuming oxygen to be the transported ion through the electrolyte). This is the general fuel reaction step taking place in all the fuel cells.

However, a theoretical alternative to steam reformation followed by hydrogen oxidation, is the *direct electrochemical oxidation* (*DEO*) of the hydrocarbons. This occurs at high temperatures directly on the fuel cell anode, where the hydrocarbons are oxidised by the oxygen ions (or carbonate ions) electrochemically transported through the electrolyte:

$$CH_4 + 4O^{2-} = CO_2 + 2H_2O + 8e^-. \quad (21)$$

The direct oxidation should allow the hydrocarbons to be completely and fully oxidised by the oxygen ions. Any competing conversion route, e.g. steam reforming or partial oxidation of the hydrocarbons in presence of steam, must be suppressed. This puts very special demands on the electrocatalytic (anode) surface, and clearly most noble metals must be avoided. Candidates could be conductive and catalytically active metal oxides. However, up to now no directly oxidising anode has been successfully demonstrated.

In order to compare these two different fuel processing routes for the medium- and high-temperature fuel cells, values for the change in free energy ΔG_T and the enthalpy change ΔH_0 must be calculated. For the reformed and shifted hydrocarbons (Eqs. (19) and (20)) the enthalpy change for the whole process ΔH_0 is

$$\Delta H_0 = \Delta H_{19} + \Delta H_{20} = \Delta H_{21}, \quad (22)$$

where the subscripts refer to the equation number. The total enthalpy is the same for both fuel processing routes, with the implicit condition that the processes in Eqs. (19) and (20) are thermally coupled (IR or DIR). The free energy that can be electrochemically utilised is however not identical for the two routes, namely ΔG_{20} for the reformed fuel and ΔG_{21} for the directly electrochemically oxidised fuel. Here ΔG_{21} is always larger than ΔG_{20}, hence the potentially higher efficiencies for the DEO-process.

The selection of a particular fuel and the following processing of the fuel do influence the fuel cell system efficiency through the parameters u_{ref} and η_{max}. Calculated values for η_{max} (see Eq. (1)) for the different fuel cell fuels, assuming both direct electrochemical oxidation and reformation of the hydrocarbons, are given in Table 2 at atmospheric pressure.

Table 2
Theoretical maximum efficiency η_{max} (LHV) (%) for a selection of different fuels at different temperatures [12][a]

Fuel	Temperature			
	80°C	200°C	650°C	1000°C
Hydrogen (H_2)	93	90	80	71
Natural gas (CH_4)				
Direct electrochemical oxidation	[b]	[b]	100	100
Thermally integrated reformation			98	89
Methanol (CH_3OH)				
Direct electrochemical oxidation	[b]	103	107	110
Thermally integrated reformation		98	88	79
Diesel (C15–C25)[c]				
Direct electrochemical oxidation	[b]		106	108
Thermally integrated reformation			95	86

[a] Values higher than 100% indicates an additional energy (heat) demand from the surrounding.

[b] External reformation of this fuel is required at this temperature, and cannot be performed thermally integrated. For maximum efficiency, see data under hydrogen as fuel.

[c] Based upon model calculations with a mixture of 64% pentadecane and 36% 1-pentylnaphthalene (both C15-hydrocarbons). This gives a H/C ratio of 1.8. For comparison, see [13].

3.2. Important parameters

The technical parameters of Eqs. (14) and (16) are parameters of interest for the user. The physical interpretation and estimated values for these parameters are given below.

- P_{max}, *the maximum power*. This parameter, or rather the combination P_{max}/A, where A is the total fuel cell active area, is a measure of the cell performance, including polarisation losses and ohmic losses in the fuel cell. From the producers' point of view a high loss factor, corresponding to a low P_{max}/A value, may be compensated with a large active fuel cell area. Hence two systems with different internal cell losses, may function with the same total system efficiency when the active fuel cell area has been adjusted.
- P_{nom}, *the nominal power output*. This is the rated maximum output power, and the dimensioning parameter for the system.
- p_{pc}, *the peak power capacity*. The peak power capacity represents the maximum, theoretical power delivery determined by the available, active fuel cell area, independent of the remaining system components.

  The peak power capacity should be as large as possible for two reasons: (i) the highest possible total efficiency, and (ii) the dynamic load following behaviour. However, since the value of this parameter is directly proportional to the effective fuel cell area for a constant output, cost considerations put a limit to the upper value. Values for p_{pc} between 130 and 180% are expected to be the preferred ones for many applications. For load following applications, see Section 3.3. Fig. 3 shows fuel cell system efficiencies for peak power capacities varying from 100 to 300%. The figure shows clearly the enhanced part power efficiency, especially at the lower p_{pc}-values.
- α_1, *the normalised stand-by losses*. The stand-by losses represent the necessary power consumed in order to maintain stand-by conditions, including: power to fans, pumps, and control unit, and thermal losses (through insulation). This parameter is likely to depend upon the stand-by (or operating) temperature, and will therefore vary from the low-temperature to the high-tempera-

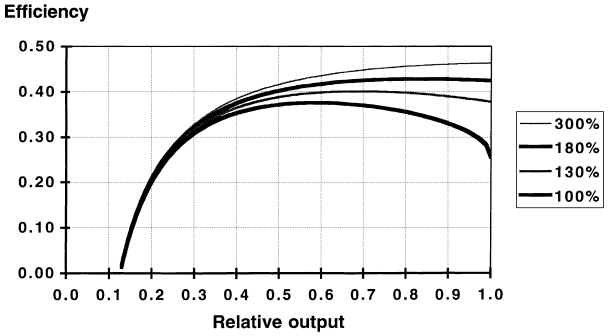

Fig. 3. System efficiency as a function of normalised power output for the PAFC of Fig. 2 with the peak power capacity (p_{pc}) as parameter, with values varying from 100 (lower graph) to 300% (upper graph). The remaining parameters have values as in Fig. 2.

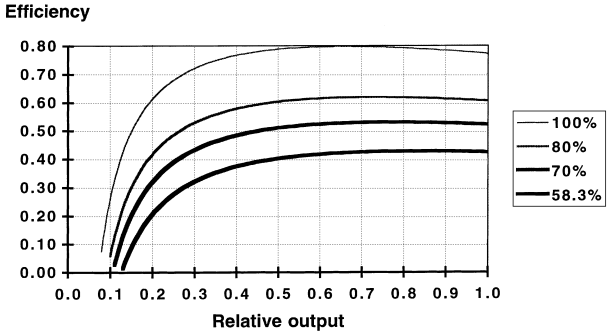

Fig. 4. System efficiency as a function of normalised power output for the PAFC of Fig. 2 with the system efficiency factor λ_0 as parameter, with values varying from 58.3 (lower graph) to 100% (upper graph). The remaining parameters have values as in Fig. 2.

ture fuel cells. With a high level of insulation, values of α_1 between 2 and 7% are expected for future developments.

- *β_0, the normalised operational dependent losses*. Similarly, the operational dependant losses cover increased losses during power generation, including: increased power to fans and pumps, and increased thermal losses due to increased stack temperature during operation. It also covers losses due to fuel and off-gas handling, and water and gas recycling.

  Values of β_0 between 5 and 10% are expected for future developments, reflecting the complexity in the handling of water and gasses in the various systems.
- u_{ref}, *reformer efficiency*. When hydrocarbons are used as fuel, fuel processing is generally necessary, at least for the low-temperature cells. According to Rostrup-Nielsen [7] modern tubular reformers have overall thermal efficiencies that approaches 95%.

  For IR and DIR, u_{ref} may be set to unity, due to the thermally integrated reformer.
- u_{fu}, *the fuel utilisation*. The fuel utilisation in the cells will for practical reasons never be 100%, because fuel depletion effects should be avoided. The value for the fuel utilisation is expected to be between 80 and 90%. The rest fuel may be catalytically burned at the fuel cell outlet or used in a bottoming cycle.
- η_{el}, *the electric conversion efficiency*. The electric conversion efficiency is expected to reach values between 90 and 97%.

  For the aggregated factors of the linearised Eq. (16), the following comments apply
- λ_0, the system *efficiency factor* has the value of 58.3% for the PAFC system [6] of Fig. 2, but is expected to reach values between 60 and 80% for future developments.

  Fig. 4 shows fuel cell system efficiencies where the efficiency factor has been varied between 58.3 and 100%, while the other parameters have values as in Fig. 2.
- λ_1, the system *first-order loss factor* has the value of −7.4% for the PAFC system [6] of Fig. 2, but is expected to be reduced to values between −3 and −6% for future developments. Fig. 5 shows fuel cell system efficiencies where the loss factor has been varied between 0 and −7.4%, while the other parameters have values as in Fig. 2.

3.3. Instantaneous load-following properties

The load-following properties are important, especially for stationary grid connected applications. Many countries that depend upon fossil fuels for their electricity generation do face challenges with respect to load following (power) capacity. Fuel cells may provide that.

Fuel cells in the 'stand-by' operational mode (working temperature achieved, gas supply active) do have the capacity of instantaneously producing electricity when turned on, although the power output is limited due to the isothermal temperature distribution in the fuel cell stack under 'stand-by' conditions. However, if the total fuel cell area is large enough for a given nominal power output, the stack will nevertheless be able to deliver sufficient electric power when turned on. The response time is determined by the time necessary to get blowers and fans up to speed. This time should be smaller than the response time experienced in hydroelectric power generation, due to the significantly larger rotational inertia of the hydroelectric equipment.

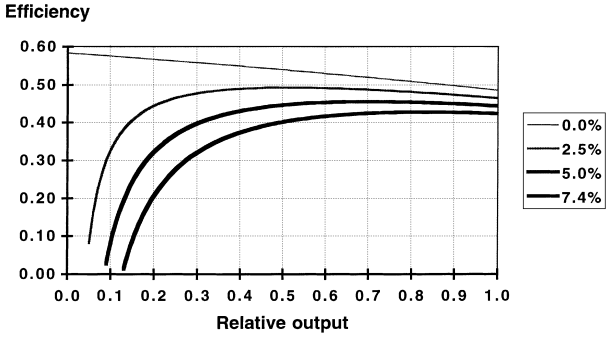

Fig. 5. System efficiency as a function of normalised power output for the PAFC of Fig. 2 with the first-order loss factor λ_1, as parameter, with values varying from −7.4 (lower graph) to 0% (upper graph). The remaining parameters have values as in Fig. 2.

Achenbach [14] and Malandrino and Manchini [15] have presented calculations on the dynamic behaviour of SOFC stacks. The most demanding situation with respect to load-following properties is when the fuel cell is in 'stand-by' position with zero power delivery. Based on Malandrino's calculations, see Appendix B, it is recommended that the peak power capacity p_{pc} exceeds 140% in order to achieve an instantaneous load-following (SOFC) fuel cell system. This in spite of the fact that the thermal time constants for a flat plate SOFC stack are of the order of 5–15 min. This condition is also likely to apply for the other fuel cell types. The only fuel cell system that can operate as a load following (or emergency back up power) system from rest — or ambient temperature — is the SPFC. This is due to its low operating temperature. However, in order to function with full power from start, the peak power capacity will have to be on the order of p_{pc} ≈200–300%, depending on the resting conditions.

3.4. Intrinsic CO_2-separation in high-temperature fuel cells

The 1997 UN conference in Kyoto on global warming, issued a number of measures in order to control the emission of the so-called 'green-house gases', of which CO_2 is the most important. CO_2 emission is unavoidable (technology independent) as long as hydrocarbons are used as fuel for energy conversion purposes. If a reduction in the CO_2 emission is required, a separation and collection of CO_2 is needed, before a further processing and/or handling (e.g. storage) can take place.

In any fuel cell system the two gas flows, fuel and air, are in principle separated throughout the system. For fuel cells running on hydrocarbon fuels, the hydrocarbon fuel may either be processed or fed directly into the cells, yielding a fuel exhaust gas consisting of CO_2 and water (according to Eqs. (19) and (20), or Eq. (21)). Water can easily be condensed, and pure CO_2 will be available at the anode outlet. On the cathode side air can be used unprocessed (80% N_2), if necessary at an over-stoichiometric ratio in order to control the stack temperature distribution. For an evaluation of the exhaust gas emission levels from fuel cell systems, see [16].

In real operating systems the fuel will never be fully consumed, but have a utilisation factor less than one. In practice this will make the cleaning somewhat more complicated (fuel after burning and/or condensation).

The fuel cell systems act as combined energy conversion and CO_2 separation devices. If a cost is set on CO_2 separation, which may be the future case due to the Kyoto Agreement, fuel cell systems will gain to their competitiveness compared with other energy conversion devices.

4. Conclusions

An analytical model for the total fuel cell system efficiency has been developed and tested on performance data from a commercial phosphoric acid fuel cell system with an acceptable fit.

This model was then used for the discussion of important fuel cell system parameters that all, in principle, should be available for the user: P_{max}/A, P_{nom}, p_{pc}, α_1, β_0, u_{ref}, u_{fu}, η_{el}, and η_{max}.

Alternatively the three important parameters p_{pc}, λ_0 and λ_1 should be available from all manufacturers of fuel cells, in addition to the nominal power output P_{nom}, and preferably the combined parameter P_{max}/A. Based upon these parameters, the basic operation of the fuel cell system can be uniquely described. Different fuel cell systems can hence be compared and evaluated for particular applications by the end user.

Finally, three useful properties of fuel cells have been focused: (i) their ability to produce electric energy with constant — or even increased — efficiency at reduced power (enhanced part power efficiency), (ii) their ability to respond instantaneously to changes in power delivery demands (instantaneous load-following properties), and (iii) their theoretical ability to deliver an exhaust gas consisting of almost pure CO_2 (intrinsic CO_2 separation).

Acknowledgements

Parts of the present work are based on contract work performed for the Commission of the European Community, under contract No. JOU2-CT93-0273. Mr. W.K.D. Borthwick is acknowledged for his encouragement to publish the work. Lars Sjunnesson is acknowledged for supplying the performance data from one of Sydkraft's PAFC test unit.

Appendix A. Asymptotic expansion of *F(p)*

From Eq. (15), the total fuel cell system efficiency (η_{TOT}) was found to yield

$$\eta_{TOT} = F(p)\frac{1+\sqrt{1-p/p_{pc}}}{2} \tag{A1}$$

where $F(p)$ is the generalised system efficiency function. The function $F(p)$ can be developed as an asymptotic series in the variable $1/p$:

$$F(p) \sim \sum_{0}^{k} \lambda_i \left(\frac{1}{p}\right)^i \quad \text{for } p \to p_0 \tag{A.2}$$

The asymptotic expansion has a limited value for k [17]. As $p_0 \to 0$, k will increase. Fig. 6 shows the calculated total system efficiency as a function of normalised power output for the PAFC-system of Fig. 2, with Eq. (A.2) expanded to three terms (a four parameter numerical model) with the values of 58.5% for the efficiency factor, 8.8% for the first-order loss factor, +0.42% for the second-order loss factor,

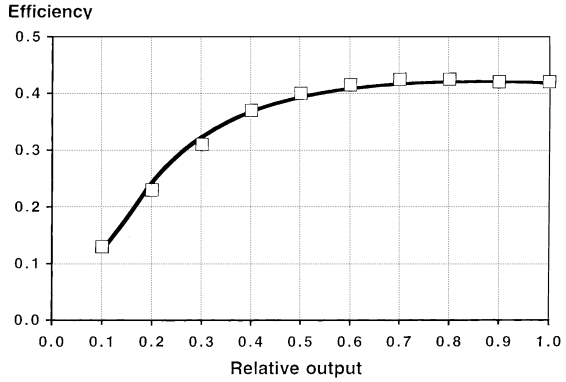

Fig. 6. Calculated fuel cell system efficiency as a function of normalised power output for the Sydkraft-system of Fig. 2, based upon the four parameter model of Eq. (A.2) with the values of 58.5% for the efficiency factor, −8.8% for the first-order loss factor, +0.42% for the second-order loss factor, and 180% for the peak power capacity.

and 180% for the peak power capacity. With these values the fit was better than ±10% for power levels down to 12% of the nominal power output.

Appendix B. Determination of the load-following values of p_{pc}

The condition for a fuel cell system to act as an instantaneously load-following power generator from 'stand-by' position, is strongly related to the value of the peak power capacity (or the active fuel cell area).

The 'stand-by' position (with zero power delivery) is characterised by a uniform temperature distribution through the fuel cell stack. In the active mode, when fuel and air is supplied to the stack, temperature will rise from the fuel inlet side towards the fuel exit side. Full power will first be achieved when the stack material temperature has reach its allowable maximum temperature distribution determined by the full fuel feed conditions.

When the fuel cell system is turned on from its 'stand-by' position, the fuel cell stack do have the capacity of instantaneously producing electric power, although the output is limited due to the isothermal temperature distribution. However, if the total fuel cell area is large enough, the stack will be able to deliver the demanded nominal power.

In order to achieve figures for the load-following condition, the work of Malandrino and Manchini [15] will be analysed. Malandrino and Manchini showed in his work that with a SOFC stack under isothermal conditions (stand-by) the SOFC stack was able to deliver an instantaneous power of approximately 1.50 kW/m^2 at a stack voltage of 0.56 V (for details, see [15]), whereas the delivered power for steady-state operation is approximately 1.86 kW/m^2 at a stack voltage of 0.62 V.

Assuming linear relationship between current and voltage, see Fig. 1, and a reversible cell voltage E_{rev} of 1.1 V, a maximum power delivery for 'stand-by' $P_{max,sb}$ can be calculated:

$$P_{max,sb} = 1.50 \times \frac{(0.55)^2}{0.56(1.1 - 0.56)} = 1.56\,\mathrm{kW/m^2} \tag{B.1}$$

whereas for the full operation, or 'steady-state' condition, a maximum power delivery ($P_{max,ss}$) can be calculated:

$$P_{max,ss} = 1.86 \times \frac{(0.55)^2}{0.62 \times (1.1 - 0.62)} = 1.89\,\mathrm{kW/m^2} \tag{B.2}$$

For a system to deliver the maximum power of 1.5 kW/m^2 even from stand-by condition, the peak power capacity (p_{pc}) determined by Eq. (5), will have to exceed

$$p_{pc} = \frac{1.89}{1.50} = 126\% \tag{B.3}$$

Eq. (B.3) gives, however, the minimum value of the peak power capacity. At start-up from 'stand-by' this will force the cell voltage to become 0.55 V. As commented by Malandrino and Manchini this voltage may be too low for the stability of the Ni-cermet anode of the SOFC. If one for stability — or other — reasons will restrict the cell voltage downward to e.g. 0.7 V, the peak power capacity (p_{pc}) will have to exceed

$$p_{pc} = \frac{1.89}{1.50} \times \frac{(0.55)^2}{0.7(1.1 - 0.7)} = 136\% \tag{B.4}$$

References

[1] W.R. Grove, Phil. Mag. 14 (1839) 127.
[2] F.T. Bacon, A.M. Adams, R.G.H. Watson, in: W. Mitchell Jr. (Ed.), Fuel Cells, Academic Press, New York, 1963.
[3] A.J. Appleby, F.R. Foulkes, Fuel Cell Handbook, Van Nostrand Reinhold, New York, 1989.
[4] K. Kinoshita, F.R. McLarnon, E.J. Cairns, Fuel Cells — A Handbook, US Department of Energy report DOE/METC-88/6096, May 1988.
[5] S.S. Penner (Ed.), Assessment of Research Needs for Advanced Fuel Cells, Pergamon Press, New York, 1986.
[6] Lars Sjunnesson, Sydkraft, Malmø, Sweden, private communication.
[7] J.R. Rostrup-Nielsen, Catal. Today 18 (1993) 305.
[8] J.R. Bang, E. Figenbaum, E. Holden, in: Proceedings of the Eurogas '92, Trondheim, Norway, 1992, p. C 87.
[9] US Congress, Office of Technology Assessment, OTA-TM-O-37, US Government Printing Office, Washington, February 1986.
[10] R.W. Glazebrook, J. Power Sources 7 (1982) 215.
[11] G.J. Baham, G. Swensson, US Department of Transportation, MA-RD-940-82028, January 1982.
[12] D.R. Stull, E.F. Westrum, G.C. Sinke, The Chemical Thermodynamics of Organic Compounds, Wiley, New York, 1969.
[13] V.W. Adams, in: Proceedings of the Second International Symposiun on SOFC, Athens, Greece, 1991, p. 247.
[14] E. Achenbach, in: U.G. Bossel (Ed.), Proceedings of the First European SOFC Forum, Lucerne, Switzerland, 1994, p. 337.
[15] A. Malandrino, N. Manchini, in: B. Thorstensen (Ed.), Proceedings of the Second European SOFC Forum, Oslo, Norway, 1996, p. 89.
[16] K.L. Seip, B. Thorstensen, H. Wang, J. Power Sources 35 (1991) 37.
[17] A. Erdélyi, Asymptotic Expansions, Dover, New York, 1956.